Proc. Natl. Acad. Sci. USA
Vol. 94, pp. 4017–4021, April 1997
Medical Sciences

KvLQT1, a voltage-gated potassium channel responsible for human cardiac arrhythmias

WEN-PIN YANG, PAUL C. LEVESQUE, WAYNE A. LITTLE, MARY LEE CONDER, FOUAD Y. SHALABY, AND MICHAEL A. BLANAR*

Department of Cardiovascular Drug Discovery, Bristol–Myers Squibb Pharmaceutical Research Institute, Route 206 and Provinceline Road, Princeton, NJ 08543-4000

Communicated by Leon E. Rosenberg, Bristol–Myers Squibb Pharmaceutical Research Institute, Princeton, NJ, January 29, 1997 (received for review November 13, 1996)

ABSTRACT **The clinical features of long QT syndrome result from episodic life-threatening cardiac arrhythmias, specifically the polymorphic ventricular tachycardia torsades de pointes. *KVLQT1* has been established as the human chromosome 11-linked gene responsible for more than 50% of inherited long QT syndrome. Here we describe the cloning of a full-length *KVLQT1* cDNA and its functional expression. *KVLQT1* encodes a 676-amino acid polypeptide with structural characteristics similar to voltage-gated potassium channels. Expression of KvLQT1 in *Xenopus* oocytes and in human embryonic kidney cells elicits a rapidly activating, K^+-selective outward current. The I_{Kr}-specific blockers, E-4031 and dofetilide, do not inhibit KvLQT1, whereas clofilium, a class III antiarrhythmic agent with the propensity to induce torsades de pointes, substantially inhibits the current. Elevation of cAMP levels in oocytes nearly doubles the amplitude of KvLQT1 currents. Coexpression of minK with KvLQT1 results in a conductance with pharmacological and biophysical properties more similar to I_{Ks} than other known delayed rectifier K^+ currents in the heart.**

Long QT syndrome (LQTS) is a cardiac disorder that causes abrupt loss of consciousness, seizures, and sudden death. Subsequent to the discovery of ion channel gene mutations that underlie specific forms of the LQTS (1–3), the molecular mechanisms of the congenital forms of LQTS have been reviewed extensively (4, 5). One locus for hereditary LQTS (LQT3) has been linked to mutations in *SCN5A* (3), a gene encoding an α-subunit of a human cardiac voltage-gated sodium channel. Another form of LQTS (LQT2) has resulted from mutations in the gene encoding HERG, the channel responsible for I_{Kr} in cardiac myocytes (2, 6, 7). Functional analysis of the mutants in both SCN5A and HERG has provided a mechanistic explanation for the prolongation of the cardiac action potential duration in LQTS patients (6–8). Here we describe the cloning and expression of a full-length cDNA clone of *KVLQT1*, the gene responsible for more than 50% of inherited LQTS (1). Pharmacological characterization of KvLQT1 and coexpression studies with minK strongly supports the hypothesis that KvLQT1 coassembles with minK to form the channel responsible for I_{Ks} currents in human cardiomyocytes.

MATERIALS AND METHODS

Molecular Cloning and Expression of *KVLQT1*. 5′ rapid amplification of cDNA ends (RACE) was performed by amplifying adult human cardiac and pancreas cDNA libraries or Marathon-Ready cDNAs (CLONTECH) using primers derived from the S1 and S2 region of the partial *KVLQT1* cDNA sequence described previously (1). PCR products were gel-purified, subcloned, and sequenced. Primers subsequently were designed from the sequences containing the candidate 5′ end of *KVLQT1* and were used for a second round of 5′ RACE. This procedure was repeated until no additional 5′ end cDNA sequence was obtained. Random-primed ^{32}P-labeled DNA probes containing specific regions of *KVLQT1* sequence were used for screening of cDNA libraries and Northern blot analysis using standard protocols. For Master blot analysis, hybridization and washing was performed as recommended by the manufacturer (CLONTECH). The full-length *KVLQT1* cDNA clone was obtained by restriction enzyme digestion and religation of two overlapping *KVLQT1* cDNA clones. Capped cRNA for microinjection was synthesized using mMESSAGE mMACHINE Kit (Ambion).

Electrophysiological and Pharmacological Characterization of KvLQT1. Stage V and VI *Xenopus* laevis oocytes were defolliculated with collagenase treatment and injected with 20 ng of *KVLQT1* cRNA, 2 ng of minK cRNA, or a combination of the two as described previously (9). Currents were recorded at room temperature using the two-microelectrode voltage clamp (Dagan TEV-200) technique between 2–6 days after injection. Microelectrodes (0.8 to 1.5 MΩ) were filled with 3 M KCl. Bath solution contained (in mM): 96 NaCl, 2 KCl, 1.8 $CaCl_2$, 1 $MgCl_2$, and 5 Hepes (pH 7.5). KCl was varied in some experiments by equimolar substitution with NaCl. Currents were recorded (Axopatch 200A) from HEK293 cells at 25°C 48–72 h after transfection. Pipettes (2–3 MΩ) were filled with internal solution containing (in mM): 125 KCl, 25 KOH, 1 $CaCl_2$, 2 $MgCl_2$, 4 K-ATP, 10 EGTA, and 10 Hepes (pH 7.2). Bath solution contained (in mM): 140 NaCl, 4 KCl, 2 $CaCl_2$, 1 $MgCl_2$, 5 Hepes, and 10 glucose (pH 7.4). Axodata and pCLAMP 6.0 (Axon Instruments) were used in oocyte and HEK293 cell experiments, respectively, for generating voltage clamp commands and acquiring data. Oocyte and HEK293 cell data was sampled at rates at least two times the low pass filter rate.

RESULTS AND DISCUSSION

To identify the 5′ end of full-length *KVLQT1*, multiple rounds of 5′-RACE PCR were performed and led to the identification

The publication costs of this article were defrayed in part by page charge payment. This article must therefore be hereby marked "*advertisement*" in accordance with 18 U.S.C. §1734 solely to indicate this fact.

0027-8424/97/944017-5$2.00/0
PNAS is available online at **http://www.pnas.org**.

Abbreviations: LQTS, long QT syndrome; RACE, rapid amplication of cDNA ends; IBMX, isobutylmethylxanthine.

Data deposition: The sequence reported in this paper has been deposited in the GenBank database (accession no. U86146).

*To whom reprint requests should be addressed at: Department of Cardiovascular Drug Discovery, Mail Code K14-01, Room K.4125A, Bristol–Myers Squibb Pharmaceutical Research Institute, Route 206 and Provinceline Road, Princeton, NJ 08543-4000. e-mail: blanar@bms.com.

of ≈500 additional nucleotides upstream of the partial *KVLQT1* cDNA sequence described previously (1). To obtain full-length cDNA clones, DNA fragments derived from the 5′ RACE-derived 5′ end of *KVLQT1* were used as a probe to screen human cardiac and pancreas cDNA libraries. A full-length cDNA clone, which contains an ORF encoding a 676-amino acid polypeptide (Fig. 1*a*), was derived from two overlapping bacteriophage clones. Nested PCR and sequencing experiments were performed to confirm that *KVLQT1* sequences from the initiation ATG codon to the 5′ end of the S1 domain were present and identical in both human cardiac and pancreas cDNA libraries. One interesting feature of the 5′ upstream sequence is its high GC content (≈80%). Because the 5′ end of *KVLQT1* is enriched for CpG dinucleotide repeats, target sites for DNA methylation, and because *KVLQT1* is located in a chromosomal region (11p15.5) known to be subject to genomic imprinting (10), it would be intriguing to determine whether *KVLQT1* is also subject to imprinting and subsequent differential expression. The total length of the composite *KVLQT1* clone is 3157 bp, which is in good agreement with the size estimated from Northern blot analysis of human poly(A)$^+$ mRNA (≈3.2 kb). When this full-length KvLQT1 amino acid sequence was subjected to BLAST analysis, significant homology (≈60% identity, 83% similarity) in the core sequences encoding the six transmembrane domains and pore region was observed to a Genefinder-predicted potassium channel-like protein, C25B8.2, from *Caenorhabditis elegans* (Fig. 1*b*). The homology extends into the amino acid sequence N terminal of the S1 domain of KvLQT1.

5′-RACE PCR experiments revealed the presence of two major 5′ splice variants: one, splice variant A, encodes the N-terminal segment of KvLQT1; the other, splice variant B, is predicted to encode a truncated protein [in which the initiation codon is only 1 amino acid away from the previously described partial *KVLQT1* sequence (1)]. The expression pattern of these two splice variants in human tissues was examined by Northern blot analysis. Probe I (Fig. 2*a*), which is common to both splice variants, was used as a control and detected a single *KVLQT1*-specific ≈3.2-kb transcript in various human tissues (Fig. 2*b*). Significantly, the splice variant A-specific probe (probe II, Fig. 2*a*) also hybridized to the ≈3.2-kb transcript in a tissue-specific expression pattern similar to that observed with probe I. This result strongly supports the notion that the ≈3.2-kb transcript encodes the functional full-length KvLQT1 protein. In addition to the ≈3.2-kb mRNA, two transcripts of ≈1.7 and ≈6.6 kb also were detected in human heart and skeletal muscle. Probe I also hybridizes faintly to these two transcripts. When the splice variant B-specific probe was used (probe III, Fig. 2*a*), a ≈3.2-kb transcript was detected in the heart and, to a lesser extent, in pancreas. Because DNA sequence analysis indicates that splice variant B encodes a truncated protein, the significance of this splice form remains to be determined. The distribution of *KVLQT1* mRNA expression, in a more extensive array of human tissues, also was determined. *KVLQT1* probe I was radiolabeled and hybridized to a human RNA Master Blot (CLONTECH; Fig. 2 *c–e*). The results are consistent with that of Northern blot analysis. Interestingly, the adrenal gland and thyroid gland exhibit much higher levels of *KVLQT1* expression than in the heart or pancreas.

The properties of the channel encoded by *KVLQT1* were investigated by injecting transcribed cRNA into *Xenopus* oocytes. Fig. 3*a* compares currents recorded from oocytes that were injected 72 h earlier with either water or 20 ng of *KVLQT1* cRNA. Oocytes injected with *KVLQT1* cRNA exhibited robust outward currents that activated at potentials positive to −60 mV and exceeded 5 μA at +40 mV (less than 150 nA at +40 mV in the water-injected oocytes). KvLQT1 currents exhibited a delayed rectifier current phenotype and rectified weakly at positive voltages. Tail currents, elicited upon repolarization to −80 mV, exhibited an initial rise in amplitude before deactivation. The initial increase in tail current amplitude may be due to fast recovery from inactivation, similar to that observed with HERG currents expressed in oocytes (6). Fig. 3*b* shows the peak current-voltage (I-V) relationship for oocytes expressing KvLQT1 (n = 12). The K^+ selectivity of the expressed current was examined by investigation of tail current reversal potentials in bath solutions containing 2, 10, 40, and 98 mM K^+. Reversal potentials closely followed the Nernst potential for K^+ (n = 6; Fig. 3*c*) revealing a highly K^+-selective channel. The dashed line has a slope predicted from the Nernst equation for a perfectly selective K^+ channel (58 mV per decade change in external K^+).

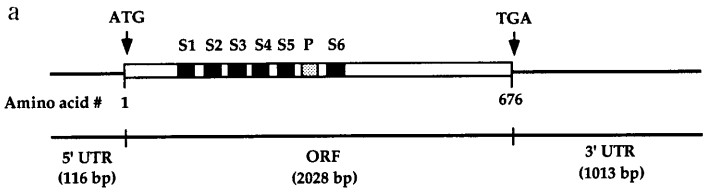

b

```
KVLQT1                          MAAASSPPRAERKRWGWGRLPGARRGSAGLAKKCPFSLELAEGGPAGGALYAPIAPGAPGPAPPASPAAPAAPPVASDLGPRPPVSLDPRVSIYSTRRPV 100

                                S1                  S2                                  S3
KVLQT1  LARTHVQGRVYNFLERPTGWKCFVYHFAVFLIVLVCLIFSVLSTIEQYAALATGTLFWMMEIVLVVFFGTEYVVRLWSAGCRSKYVGLWGRLRFARKPISIIDLIVVVASMVVLCVGSKGQ 220
C25B8.2 ...RRMQNKMHNFLERPRGWKAATYHLAVLFMVLMCLALSVFSTMPDFEVNATIVLYYLEIVFVIWLATEYICRVWSAGCRSRYRGISGRIRFATSAYCVIDIIVILASITVLCIGATGQ 222

        S4                              S5                                  P                   S6
KVLQT1  VFATSAIRGIRFLQILRMLHVDRQGGTWRLLGSVVFIHRQELITTLYIGFLGLIFSSYFVYLAEKDAVNESGRVEFGSYADALWWGVVTVTTIGYGDKVPQTWVGKTIASCFSVFAISFF 340
C25B8.2 VFAASAIRGLRFFQILRMLRIDRRAGTWKLLGSVVWAHRQELLTTVYIGFLGLIFSSFLVYLCEKNT-ND--K--YQTFADALWWGVITLSTVGYGDKTPETWPGKIIAAPCALLGISFF 337

        ALPAGILGSGFALKVQQKQRQKHFNRQIPAAASLIQTAWRCYAAENPDSSTWKIYIRKAPRSHTLLSPSPKPKKSVVVKKKKFKLDKDNGVTPGEKMLTVPHITCDPPEERRLDHFSVDG 460
C25B8.2 ALPAGILGSGFALKVQQHQRQKHLIRRRVPAAKLIQCLWRHYSAA-PESTSLATWKIHL... 395

KVLQT1  YDSSVRKSPTLLEVSMPHFMRTNSFAEDLDLEGETLLTPITHISQLREHHRATIKVIRRMQYFVAKKKFQQARKPYDVRDVIEQYSQGHLNLMVRIKELQRRLDQSIGKPSLFISVSEKS 580

KVLQT1  KDRGSNTIGARLNRVEDKVTQLDQRLALITDMLHQLLSLHGGSTPGSGGPPREGGAHITQPCGSGGSVDPELFLPSNTLPTYEQLTVPRRGPDEGS*                       676
```

FIG. 1. Isolation of a full-length *KVLQT1* cDNA. (*a*) A full-length human *KVLQT1* cDNA (3,157 bp) was derived from two overlapping λgt11 cDNA clones. S1–S6, transmembrane domains 1 through 6; P, pore-forming domain; ORF, open-reading frame; 5′ UTR and 3′ UTR, 5′ and 3′ untranslated regions, respectively. The figure is not drawn to scale. (*b*) Amino acid sequence of KvLQT1 and comparison to a Genefinder-predicted potassium channel-like protein, C25B8.2, from *C. elegans* (GenBank database accession no. U41556). | denotes amino acid sequence identity; : denotes a conservative amino acid substitution.

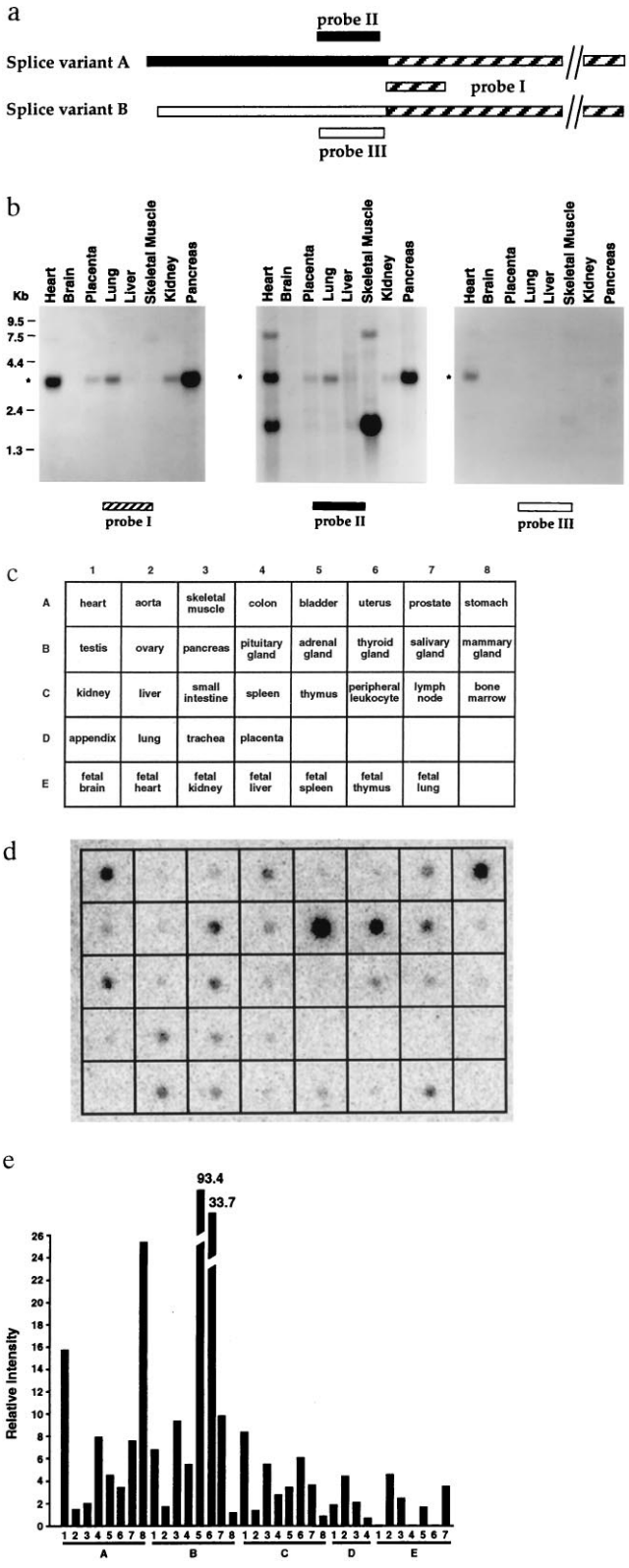

FIG. 2. Expression of KvLQT1 in human tissues. (*a*) The relative positions of the *KVLQT1* probes used for Northern blot analysis. Probe I contains nucleotide sequences derived from amino acids 130–207, whereas probe II was derived from amino acids 49–128 (Fig. 1). The sequence of probe III is upstream of the published *KVLQT1* partial sequence (1) and is totally different from that of probe II. (*b*) Poly(A)$^+$ mRNA Northern blots were hybridized individually to radiolabeled probes derived from the S1-S3 domain (probe I), the splice variant A-specific sequence (probe II), and the splice variant B-specific sequence (probe III) as indicated. RNA molecular weight markers are indicated on the left. * denotes the 3.2-kb *KVLQT1* mRNA. (*c*) Type and position of human poly(A)$^+$ mRNAs on a human RNA Master blot (CLONTECH). (*d*) Hybridization of radiolabeled *KVLQT1* probe I to a human RNA Master blot (CLONTECH). (*e*) Relative expression of *KVLQT1* mRNA in various human tissues.

Inhibitors of known voltage-gated delayed rectifier currents present in cardiac myocytes were used to investigate the pharmacology of KvLQT1. The effects of 10 μM E-4031, 2 mM 4-aminopyridine (4-AP), 10 mM tetraethylammonium, and 10 μM clofilium on KvLQT1 currents recorded from a single oocyte are shown in Fig. 3*d*. Tetraethylammonium, a weak inhibitor of I_{Ks} (11), and clofilium, an inhibitor of both I_{Kr} and I_{Ks} (12, 13), inhibited KvLQT1 current. In separate experiments, tetraethylammonium (10 mM) and clofilium (10 μM) inhibited KvLQT1 currents, recorded at +30 mV, by 20.2 $\pm$ 2.6% (n = 4) and 69.6 $\pm$ 5.7% (n = 6), respectively. E-4031, a selective inhibitor of I_{Kr} (14), and 4-AP, an inhibitor of I_{Kur} (15), produced no significant effects on KvLQT1 current, even when a repetitive pulse protocol was used (n = 4). Dofetilide (1 μM), another selective I_{Kr} inhibitor (16), also failed to block KvLQT1 current (n = 3) during a repetitive pulse protocol. The pharmacology of KvLQT1 most closely resembles that of I_{Ks} because clofilium, but not dofetilide, E-4031, or 4-AP, blocks KvLQT1 current. The fact that LQTS patients are more likely to develop serious ventricular arrhythmias under sympathetic activation has led to the suggestion that ion channels, regulated by β-adrenergic stimulation, may play a role in the pathogenesis of LQTS (5). To test the effect of elevated cAMP levels on KvLQT1 function, forskolin and isobutylmethylxanthine (IBMX), which activate adenylate cyclase and inhibit phosphodiesterase respectively, were applied simultaneously to KvLQT1-injected oocytes. As shown in Fig. 3*e*, these agents nearly double the amplitude of KvLQT1 currents. Currents stimulated by forskolin and IBMX were recorded in five other KvLQT1-injected oocytes and never in controls. Thus, although the relationship to the disease remains to be clarified, we have shown that a channel involved in LQTS indeed is regulated by sympathetic stimulation. Interestingly, slowly activating delayed rectifier currents (I_{Ks}) recorded from oocytes injected with cRNA encoding minK also are stimulated by cAMP (17).

Although KvLQT1 currents in oocytes do not match known currents native to cardiac myocytes precisely, the pharmacology and regulation by cAMP suggests that KvLQT1 most closely resembles I_{Ks}. However, the current elicited by KvLQT1 in oocytes clearly activates more rapidly than I_{Ks}. To address the possibility that the oocyte environment may alter the properties of KvLQT1, the clone was expressed transiently in human embryonic kidney (HEK293) cells. Families of voltage-gated currents recorded from plasmid control- and KvLQT1-transfected HEK293 cells are compared in Fig. 4*a* and *b*. Endogenous outward currents in plasmid control-transfected cells activated at potentials positive to -10 mV and ranged from 0.1–0.4 nA at +60 mV (n = 12). Endogenous currents displayed fast activation and slow inactivation and importantly, never had measurable tail currents (18). In KvLQT1-transfected cells, depolarizations to potentials positive to -50 mV elicited outward currents that activated more slowly than endogenous currents and ranged from 0.9–2.1 nA at +60 mV (n = 7). The kinetics of the KvLQT1 currents recorded from oocytes and HEK293 cells were similar. Amiodarone (10 μM) inhibited outward currents in cells expressing KvLQT1, but not in control-transfected cells (Fig. 4 *a* and *b*). Inhibition by amiodarone, a class III agent that blocks I_{Ks} (19), was calculated from peak tail current measurements, because tail currents were never observed in mock-transfected cells (18). Peak tail currents were inhibited by 50–60% in KvLQT1-expressing cells (n = 3). Interestingly, the IC_{50} for amiodarone against I_{Ks} in guinea pig ventricular myocytes is 10 μM (19).

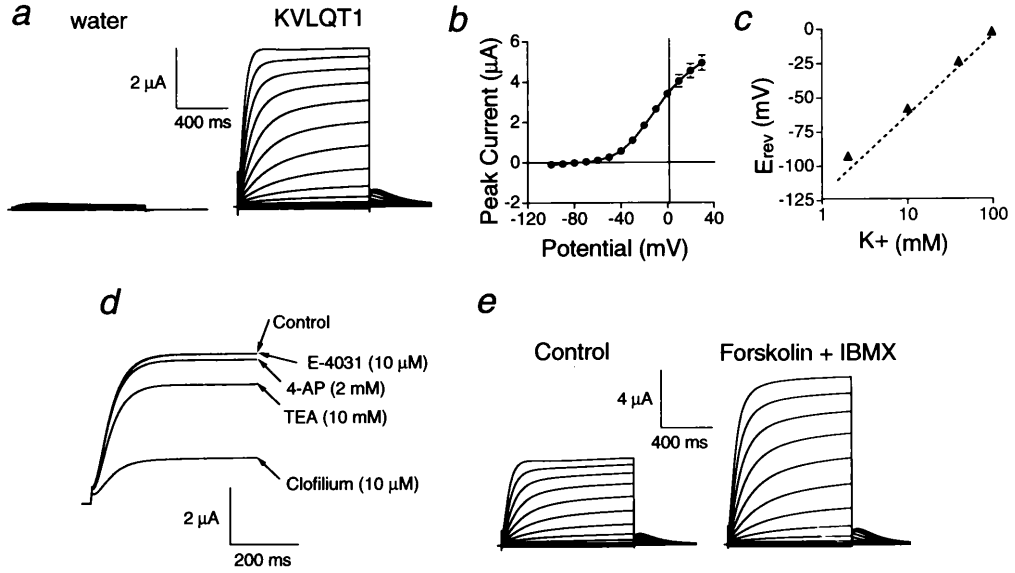

FIG. 3. Functional and pharmacologic characterization of KvLQT1 currents in *Xenopus* oocytes. (*a*) Families of currents from water- and KvLQT1-injected oocytes were elicited by 1-sec voltage steps from a holding potential of −80 mV to test potentials ranging from −100 to +40 mV in 10 mV increments. (*b*) Peak current-voltage (I-V) relationship for 12 oocytes expressing KvLQT1. Currents were recorded using the protocol in *a*. (*c*) Dependence of tail current reversal potential (E_{rev}) on the external K^+ concentration. Tail currents were elicited at potentials of −110 to +10 mV after a pulse to +20 mV (n = 6 oocytes), while the external K^+ concentration was varied between 2, 10, 40, and 98 mM. E_{rev} under each condition was determined for each oocyte by measuring the zero intercept from a plot of tail current amplitude versus test potential. The dashed line has a slope of 58 mV and is drawn according to the Nernst equation for a perfectly selective K^+ channel. Data are the mean ± SEM from six experiments. (*d*) Effects of E-4031, 4-aminopurine, tetraethylammonium, and clofilium on KvLQT1 current. Superimposed currents were recorded during 500-ms steps to +30 mV, from −80 mV, during the same experiment. Compounds were applied via bath perfusion in order from top to bottom. The bath was perfused with control solution for 5 min, or until effects reversed completely, between compounds. (*e*) Effects of cAMP on KvLQT1 currents. Currents were recorded using the protocol in *a* before and 10 min after the simultaneous addition of 10 μM forskolin and 100 μM IBMX to the bath.

Neither E-4031 (3 μM) nor dofetilide (1 μM) inhibited KvLQT1 currents in HEK293 cells (n = 3 each; data not shown). Thus, whereas KvLQT1 currents are insensitive to selective inhibitors of I_{Kr} in both oocytes and HEK293 cells, KvLQT1 currents are blocked by inhibitors of I_{Ks}.

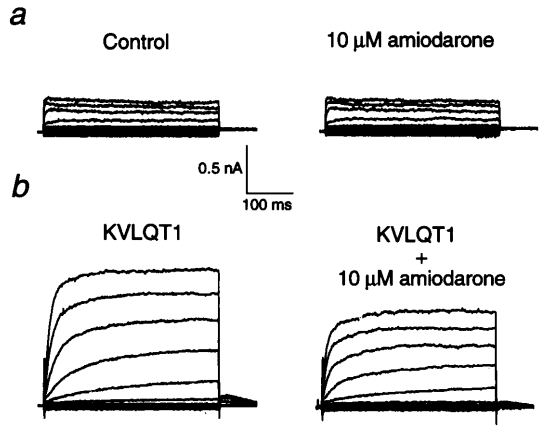

FIG. 4. Characterization of KvLQT1 currents transiently expressed in HEK293 cells. (*a*) Endogenous currents in plasmid control-transfected cells elicited by 400-ms steps, from −80 mV, to potentials between −120 and +60 mV (20 mV increments). No discernible differences in currents are observed 5 min after bath application of 10 μM amiodarone. No tail currents are discernible at −80 mV, nor are they detected when voltage is stepped back to −60 or −40 mV. (*b*) Family of KvLQT1 currents, elicited using the protocol in *a*, before and 2 min after bath addition of 10 μM amiodarone. Depolarization-induced outward currents were observed 1–2 min after addition of 10 μM amiodarone via the bath. Tail currents were measured to quantify the effect of amiodarone, because they were observed only in HEK293 cells expressing KvLQT1 and never in control cells. Amiodarone reduced peak tail current amplitude at −60 mV by 51% in the cell shown.

The electrophysiologic and pharmacologic properties of KvLQT1 alone are similar in both oocytes and HEK293 cells and cannot be positively matched to any known native current in cardiac myocytes. Although the pharmacological properties of KvLQT1 are similar to those of I_{Ks}, their kinetics of activation differ considerably. Because ion channels can be modulated through their interaction with other subunits (20), an interesting possibility is that KvLQT1 associates with the minK polypeptide to form the channel responsible for the I_{Ks} current. MinK, the gene believed to encode cardiac I_{Ks} (11, 21, 22), was a logical candidate given the debate as to whether minK encodes a K+ channel as a homomultimer, whether it associates with a separate ancillary protein or subunit, or whether minK merely regulates the activity of another channel protein (23). To test for the interaction, *KVLQT1* cRNA was coinjected with minK cRNA into *Xenopus* oocytes and membrane currents were recorded (Fig. 5*a*). The time course of activation of KvLQT1 is altered by the coexpression of minK, resulting in a slowly activating current more similar to I_{Ks}. Tail currents were small because the voltage was stepped back to −80 mV after test pulses. Current amplitudes recorded during voltage steps to positive potentials were consistently 20-fold greater in oocytes coinjected with both minK and KvLQT1 than in oocytes expressing minK alone. MinK current in different oocytes rarely exceeded 0.5 μA at +40 mV, whereas minK+KvLQT1 currents were usually greater than 10 μA at the same potential. The peak IV relationship reveals that the activation threshold for minK+KvLQT1 current (Fig. 5*b*) is shifted by nearly 20 mV positive to the activation threshold of KvLQT1 current (Fig. 3*b*) and is more consistent with I_{Ks} (14, 16). Clofilium was much less effective in inhibiting minK+KvLQT1 (Fig. 5*c*) compared with KvLQT1 alone (Fig. 3*d*). Clofilium (30 μM) reduced minK+KvLQT1 peak currents recorded during voltage steps (3 s) from −80 mV to +30 mV by 20.6 + 7.1% (n = 4), whereas the same concentration of clofilium reduced KvLQT1 currents by 80–90% in a separate

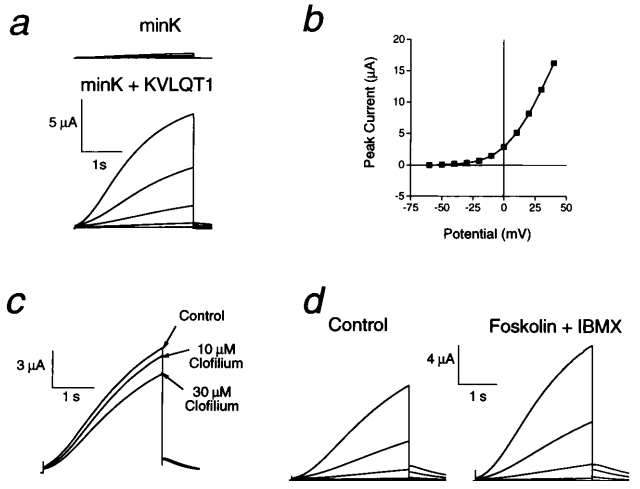

FIG. 5. Functional and pharmacological characterization of minK+KvLQT1 currents in *Xenopus* oocytes. (*a*) Families of currents from minK- and minK+KvLQT1-injected oocytes elicited by 3-s voltage steps from a holding potential of −80 mV to test potentials ranging from −40 to +40 mV (20 mV increments). Voltage was returned to the original holding potential after the voltage steps. Currents were recorded 3 days after injecting cRNAs. Peak outward current amplitudes at +40 mV in minK-injected and minK+KvLQT1-injected oocytes were 0.5 and 10.3 μA, respectively. (*b*) Peak current voltage relationship for six oocytes expressing minK+KvLQT1. Currents were elicited 4 days after injecting oocytes by 3-s voltage steps from −80 mV to potentials ranging from −60 to +40 mV. (*c*) Effects of clofilium on minK+KvLQT1 current. Superimposed currents were recorded during 3-s steps to +30 mV from −80 mV during the same experiment. Clofilium was applied via bath perfusion. (*d*) Effects of forskolin and IBMX on minK+KvLQT1 currents. Currents were recorded during 3-s voltage steps from −80 mV to potentials between −50 and +30 mV (20 mV increments). Tail currents were elicited by stepping back to −70 mV. Currents were recorded before and 10 min after adding 10 μM forskolin and 100 μM IBMX to the bath.

experiment (data not shown). The clofilium sensitivity of minK+KvLQT1 is more similar to that of minK (11, 21) and I_{Ks} (12, 13) for which the IC_{50} for clofilium is close to 100 μM. MinK+KvLQT1 peak currents were stimulated by 44% with the addition of 10 μM forskolin and 100 μM IBMX (Fig. 5*d*). The degree of stimulation by these agents at 10 min varied between 35% and 95% in five oocytes.

Coexpression of minK with KvLQT1 results in a conductance with pharmacological and biophysical properties more closely resembling I_{Ks} than does the current observed in oocytes expressing KvLQT1 alone. Our results support the hypothesis that KvLQT1 and minK coassemble *in vivo* and form the channel responsible for the cardiac I_{Ks} current. Recently, while this report was in review, two groups also have described the functional interaction of KvLQT1 and minK (24, 25). Although the consequences of *KVLQT1* mutations on channel function have not yet been reported, it is reasonable to hypothesize that these mutations reduce I_{Ks}, resulting in cardiac action potential prolongation and an increased risk of ventricular tachyarrhythmias.

Note Added in Proof. Recently, Lee *et al*. (26) demonstrated that the human *KVLQT1* gene is imprinted in a tissue-specific manner and encodes multiple mRNA splice isoforms. Isoform 1 of Lee *et al*. is equivalent to our splice variant A; isoform 2 is equivalent to our splice variant B. As described by Lee *et al*., "Isoform 1 must also contain additional upstream exons as it lacks an initiating methionine codon." Here, we describe the full-length isoform 1 cDNA.

We thank B. Kienzle, L. Gelbert, N. Thomson, and T. Nelson for DNA sequencing; T. Jenkins-West for oocyte preparation and expert technical assistance; B. Gavin and N. Lodge for comments on the manuscript; and W. Koster and D. Hathaway for discussion, comments, and support. This work was supported by the Bristol–Myers Squibb Pharmaceutical Research Institute.

1. Wang, Q., Curran, M. E., Splawski, I., Burns, T. C., Millholland, J. M., VanRaay, T. J., Shen, J., Timothy, K. W., Vincent, G. M., Jager, T. D., Schwartz, P. J., Towbin, J. A., Moss, A. J., Atkinson, D. L., Landes, G. M., Conners, T. D. & Keating, M. T. (1996) *Nat. Genet.* **12,** 17–23.
2. Curran, M. E., Splawski, I., Timothy, K. W., Vincent, G. M., Green, E. D. & Keating, M. T. (1995) *Cell* **80,** 795–803.
3. Wang, Q., Shen, J., Splawski, I., Atkinson, D., Li, Z., Robinson, J. L., Moss, A. J., Towbin, J. A. & Keating, M. T. (1995) *Cell* **80,** 805–811.
4. Roden, D. M., Lazzara, R., Rosen, M., Schwartz, P. J., Towbin, J. & Vincent, G. M. (1996) *Circulation* **94,** 1996–2012.
5. Kass, R. S. & Davies, M. P. (1996) *Cardiovasc. Res.* **32,** 443–454.
6. Sanguinetti, M. C., Jiang, C., Curran, M. E. & Keating, M. T. (1995) *Cell* **81,** 299–307.
7. Sanguinetti, M. C., Curran, M. E., Spector, P. S. & Keating, M. T. (1996) *Proc. Natl. Acad. Sci. USA* **93,** 2208–2212.
8. Bennett, P. B., Yazawa, K., Makita, N. & George, A. L., Jr. (1995) *Nature (London)* **376,** 683–685.
9. Levesque, P. C., Hart, P. J., Hume, J. R., Kenyon, J. L. & Horowitz, B. (1992) *Circ. Res.* **71,** 1002–1007.
10. Issa, J.-P. J. & Baylin, S. B. (1996) *Nat. Med.* **2,** 281–282.
11. Honoré, E., Attali, B., Romey, G., Heurteaux, C., Ricard, P., Lesage, F., Lazdunski, M. & Barhanin, J. (1991) *EMBO J.* **10,** 2805–2811.
12. Arena, J. P. & Kass, R. S. (1988) *Mol. Pharmacol.* **34,** 60–66.
13. Colatsky, T. J., Follmer, C. H. & Starmer, C. F. (1990) *Circulation* **82,** 2235–2242.
14. Sanguinetti, M. C. & Jurkiewicz, N. K. (1990) *J. Gen. Physiol.* **96,** 195–215.
15. Wang, Z., Fermini, B. & Nattel, S. (1993) *Circ. Res.* **73,** 1061–1076.
16. Jurkiewicz, N. K. & Sanguinetti, M. C. (1993) *Circ. Res.* **72,** 75–83.
17. Blumenthal, E. M. & Kaczmarek, L. K. (1992) *J. Neurosci.* **12,** 290–296.
18. Snyders, D. J. & Chaudhary, A. (1996) *Mol. Pharmacol.* **49,** 949–955.
19. Balser, J. R., Bennett, P. B., Hondeghem, L. M. & Roden, D. M. (1991) *Circ. Res.* **69,** 519–529.
20. Deal, K. K., England, S. K. & Tamkun, M. M. (1996) *Physiol. Rev.* **76,** 49–67.
21. Folander, K., Smith, J. S., Antanavage, J., Bennett, C., Stein, R. B. & Swanson, R. (1990) *Proc. Natl. Acad. Sci. USA* **87,** 2975–2979.
22. Varnum, M. D., Busch, A. E., Bond, C. T., Maylie, J. & Adelman, J. P. (1993) *Proc. Natl. Acad. Sci. USA* **90,** 11528–11532.
23. Ben-Efraim, I., Shai, Y. & Attali, B. (1996) *J. Biol. Chem.* **271,** 8768–8771.
24. Barhanin, J., Lesage, F., Guillemare, E., Fink, M., Lazdunski, M. & Romey, G. (1996) *Nature (London)* **384,** 78–80.
25. Sanguinetti, M. C., Curran, M. E., Zou, A., Shen, J., Spector, P. S., Atkinson, D. L. & Keating, M. T. (1996) *Nature (London)* **384,** 80–83.
26. Lee, M. P., Hu, R.-J., Johnson, L. A. & Fineberg, A. P. (1997) *Nat. Genet.* **15,** 181–185.